


Article

Influence of ZnF₂ and WO₃ on Radiation Attenuation Features of Oxyfluoride Tellurite WO₃-ZnF₂-TeO₂ Glasses Using Phy-X/PSD Software

Aljawhara H. Almuqrin¹ and M. I. Sayyed^{2,3,*} 

¹ Department of Physics, College of Science, Princess Nourah bint Abdulrahman University, P.O. Box 84428, Riyadh 11671, Saudi Arabia; ahalmoqren@pnu.edu.sa

² Department of Physics, Faculty of Science, Isra University, Amman 11622, Jordan

³ Department of Nuclear Medicine Research, Institute for Research and Medical Consultations (IRMC), Imam Abdulrahman bin Faisal University (IAU), P.O. Box 1982, Dammam 31441, Saudi Arabia

* Correspondence: dr.mabualssayed@gmail.com

Abstract: The radiation shielding features of the ternary oxyfluoride tellurite glasses were studied by calculating different shielding factors. The effect of the TeO₂, WO₃, and ZnF₂ on the tested glass system's attenuating performance was predicted from the examination. The mass attenuation coefficient (μ/ρ) values for the oxyfluoride tellurite glasses depend highly on the concentration of WO₃, as well as ZnF₂. All the present ZnFWTe1-ZnFWTe5 samples have higher μ/ρ values than that of the pure TeO₂ glass at all energies. For the samples with a fixed content of WO₃, the replacement of TeO₂ by ZnF₂ increases the μ/ρ , while for the glasses with a fixed content of TeO₂, the replacement of WO₃ by ZnF₂ results in a decline in the μ/ρ values. The results revealed that ZnFWTe4 has the lowest linear attenuation coefficient (μ) among the oxyfluoride tellurite glasses, whereby it has a slightly higher value than pure TeO₂ glass. The maximum effective atomic number (Z_{eff}) is found at 0.284 MeV and varied between 31.75 and 34.30 for the tested glasses; it equaled to 30.29 for the pure TeO₂ glass. The half-value layer (HVL) of the glasses showed a gradual decline with increasing density. The pure TeO₂ was revealed to have thicker HVL than the selected oxyfluoride tellurite glasses. A 1.901-cm thickness of the sample, ZnFWTe1, is required to decrease the intensity of a photon with an energy of 0.284 MeV to one-tenth of its original, whereas 1.936, 1.956, 2.212, and 2.079 cm are required for glasses ZnFWTe2, ZnFWTe3, ZnFWTe4, and ZnFWTe5, respectively.

Keywords: oxyfluoride tellurite glasses; gamma radiation; attenuation



Citation: Almuqrin, A.H.; Sayyed, M.I. Influence of ZnF₂ and WO₃ on Radiation Attenuation Features of Oxyfluoride Tellurite WO₃-ZnF₂-TeO₂ Glasses Using Phy-X/PSD Software. *Materials* **2022**, *15*, 2285. <https://doi.org/10.3390/ma15062285>

Academic Editors: Pengfei Wang, Richard Martin and Wieslaw Strek

Received: 29 January 2022

Accepted: 16 March 2022

Published: 19 March 2022

Publisher's Note: MDPI stays neutral with regard to jurisdictional claims in published maps and institutional affiliations.



Copyright: © 2022 by the authors. Licensee MDPI, Basel, Switzerland. This article is an open access article distributed under the terms and conditions of the Creative Commons Attribution (CC BY) license (<https://creativecommons.org/licenses/by/4.0/>).

1. Introduction

In the current century, radiation protection is becoming mandatory for non-ionizing radiation, such as infrared and microwave, as well as for ionizing radiation in several technological applications. Hence, it is necessary to perform empirical research that determines the shielding properties of several materials. In the construction of nuclear and industrial facilities where radioisotopes are planned for utilization, apart from the architectural design and the normally evaluated mechanical, thermal, and physical features of the materials used in the construction, their photon-shielding characteristics are also important [1–4]. Radiation-shielding factors for the constructing facilities where gamma rays are used should be accurately determined and reported. Concrete is one of the most traditional materials utilized to shield from ionizing radiation, especially in medical applications, where X-rays are used in diagnosing patients [5]. Moreover, several kinds of rocks have been developed as radiation protection materials at different gamma energies from several keV to 10 MeV [6]. Moreover, glasses have been developed recently and utilized as promising shielding materials [7–10].

The comparatively cheap cost of preparing the glasses, their ability to be fabricated into any shape according to the applications, as well as their diverse methods for preparation and notably good photon attenuation coefficients make them attractive materials for shielding aims [11–14]. The gamma rays' shielding tendency of glasses is directly related to their density, hence glasses prepared with heavy metal oxides, such as PbO, WO₃, Sb₂O₃, and Bi₂O₃, can appropriately be used as gamma ray shields [15–18]. Moreover, different works have demonstrated that the thicknesses of the glass sample can be reduced by using certain types of heavy metal oxides with an appropriate composition. TeO₂-based glass systems are a subject of interest for investigators, materials engineers, and glasses developers, due to their interesting physical and chemical characteristics such as a large transparency window, high linear and non-linear refractive indexes, low phonon frequency, and good photons' attenuation ability [19]. Oxyfluoride glass systems, including those based on TeO₂, are also important objects.

Incorporation of metal fluorides to the tellurite systems may improve the physical properties for the resulting glass systems. The estimation of gamma photons' attenuation factors for the oxyfluoride glass systems is very useful for the development of novel shielding glasses. There are several techniques to estimate the photon attenuation factors for any shields, such as: (a) Experimental methods using the transmission geometry technique or any other appropriate setup; (b) the numerical method, including different Monte Carlo simulation codes; and (c) the theoretical approach, using some common software [20–22]. In this research work, the radiation-shielding features of the WO₃-ZnF₂-TeO₂ glasses were studied by calculating different shielding factors using the Phy-X/PSD software. Moreover, the role of the TeO₂, WO₃, and ZnF₂ on the attenuating performance of the tested samples was predicted.

2. Materials and Method

It is well known that the gamma-ray attenuating characteristics of any medium depends on its composition and its density. For multi-component glass samples (such as the tested ternary oxyfluoride tellurite glasses), the mass attenuation coefficient (μ/ρ) can be found using Equation (1):

$$(\mu/\rho)_{glass} = \sum_i w_i (\mu/\rho)_i \quad (1)$$

In the above formula: w_i is the respective weight fraction of the i th component (in this study, w_i denotes the weight fraction of Zn, O, F, Te, and W). The linear attenuation coefficient (μ) is another factor that indicates the fraction of attenuated gamma rays when they pass into a medium. It is measured in a unit of cm⁻¹ or mm⁻¹. It is a density-dependent parameter and also an energy-dependent parameter. The aforementioned parameter is important, as it helps in determining other shielding parameters, such as the half value layer (HVL). It represents the width of the shield, where 50% of the incoming radiation has been attenuated [23]. Similar to μ , HVL is photon energy-dependent. The following formula is used for the evaluation of the HVL of any attenuator:

$$HVL = \frac{0.693}{\mu} \quad (2)$$

Moreover, the mean free path (MFP) is another factor used by the shielding glasses developers to estimate the distance that the photons travel into the glass sample between collisions [24]. For practical utilization, especially where space is restricted, a glass sample with a small HVL, as well as MFP, is preferable. This can be obtained using dense samples that contain heavy metal oxides, such as WO₃ and TeO₂. For the tested WO₃-ZnF₂-TeO₂ glasses, the following formula can be used for the evaluation of MFP:

$$MFP = \frac{1}{\mu} \quad (3)$$

Moreover, for the selected oxyfluoride tellurite glasses, the researcher determined the effective atomic number (Z_{eff}). This describes the interaction of radiation with composite materials. High Z_{eff} values for the sample imply the good shielding ability of the sample. The Z_{eff} for the tested oxyfluoride tellurite glasses was evaluated using Phy-X/PSD computer program [25]. This is a recently launched friendly online software that can estimate several radiation-shielding factors (such as Z_{eff}) in the continuous energy region or chosen energy values (such as the energies emitted from the common radioisotopes). Any researcher can find this software online at <https://phy-x.net/PSD> (accessed on 1 January 2021).

In short, the method for the calculations of any shielding parameters for a certain sample using this software can be summarized as follows: (i) definition of the sample: the user must define the composition of the sample with its density. This is available in the software by using either the weight fraction or mole fraction. The weight (mole) fractions must equal to 1 (100). In this program, the user can define an unlimited number of samples at the same time by using the symbol (+) in the main screen of the program. The second step (ii) selection of the investigated energies: in this step, the user can define the energies at a wide energy range, such as 15 keV–15 MeV and 1 keV–100 GeV, or at some energies emitted from common radioisotopes, such as 0.356 MeV, 0.662 MeV, and 1.173 MeV. The third step (iii) selection of the parameters to be evaluated: in this software, the user can determine several parameters related to the radiation shielding at the same time. After these three steps, users can save the results in a Microsoft Office Excel file for further discussion and analysis. More details about the application language, main screen interface, and flow chart for this software are available in Ref. [25].

The compositions of the investigated glasses are listed in Table 1 [19,26]. Moreover, featured in the same table, is the density of the pure TeO₂ glass. The selected samples were labeled as 'ZnFWTe1', 'ZnFWTe2', 'ZnFWTe3', 'ZnFWTe4', and 'ZnFWTe5', respectively, for convenience.

Table 1. Composition of the chosen ZnF₂–WO₃–TeO₂ glass system.

Sample Code	ZnF ₂	WO ₃	TeO ₂	Density (g/cm ³)
ZnFWTe1	10	20	70	5.94
ZnFWTe2	20	20	60	5.90
ZnFWTe3	30	20	50	5.91
ZnFWTe4	20	10	70	5.72
ZnFWTe5	25	15	60	5.81
Pure TeO ₂ glass				4.806

3. Results and Discussion

The μ/ρ values have been evaluated by applying the Phy-X software at eight energies between 0.284–2.506 MeV (see Figure 1). Moreover, the μ/ρ for the pure TeO₂ glass at the investigated energies is plotted in the same figure. As expected, the μ/ρ for the chosen glasses depends highly on the concentration of WO₃, as well as ZnF₂. All the ZnFWTe1–ZnFWTe5 samples have higher μ/ρ values than that of the pure TeO₂ glass. At 0.284 MeV, the μ/ρ values are 0.204, 0.202, 0.199, 0.182, and 0.191 cm²/g for ZnFWTe1, ZnFWTe2, ZnFWTe3, ZnFWTe4, and ZnFWTe5, respectively. Meanwhile, the μ/ρ for the pure TeO₂ glass at this energy is 0.168 cm²/g.

In addition, at 0.826 MeV, the μ/ρ for the ZnFWTe1–ZnFWTe5 glasses are 0.0683, 0.0685, 0.0686, 0.0669, and 0.0678 cm²/g; whereas, for the pure TeO₂ glass, it is 0.0652 cm²/g. From Figure 1, it can also be noted that for the samples with a fixed content of WO₃ (namely ZnFWTe1, ZnFWTe2, and ZnFWTe3, which contain 20 mol% of WO₃), the replacement of TeO₂ by ZnF₂ increases the μ/ρ , which is correct at all energies except at 0.284 MeV. Hence, the researcher found that $(\mu/\rho)_{\text{ZnFWTe3}} > (\mu/\rho)_{\text{ZnFWTe2}} > (\mu/\rho)_{\text{ZnFWTe1}}$. On the

other hand, for the glasses with a fixed content of TeO_2 (namely ZnFWTe1 and ZnFWTe4, which contain 70 mol% of TeO_2), the replacement of WO_3 by ZnF_2 led to a decrease in the μ/ρ values. For instance, at 1.173 MeV, the μ/ρ for ZnFWTe1 and ZnFWTe4 are 0.0546 and 0.0541 cm^2/g . For the samples with a fixed concentration of ZnF_2 (i.e., ZnFWTe1 and ZnFWTe4), the decrease in WO_3 content leads to a reduction in the μ/ρ values. The change in the μ/ρ may be ascribed to the μ/ρ of the constituent component, wherein the general WO_3 has higher μ/ρ values than that of TeO_2 and ZnF_2 , while ZnF_2 has the smallest μ/ρ .

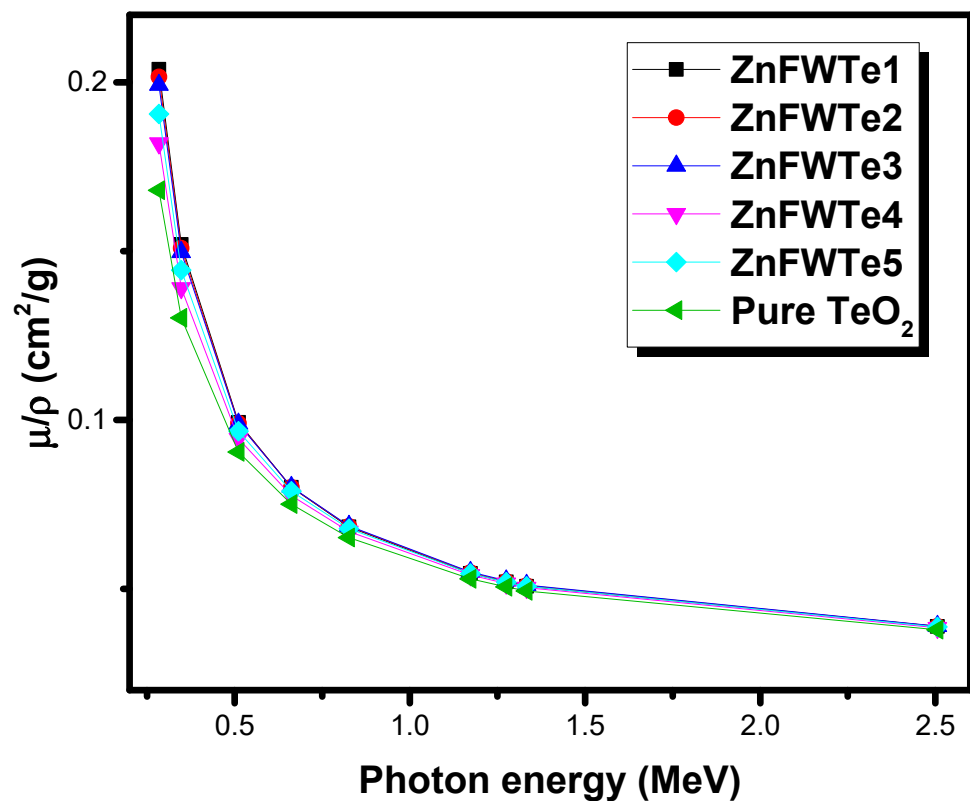


Figure 1. The mass attenuation coefficient for the oxyfluoride tellurite glasses.

Notwithstanding, the μ can be utilized to deduce the fractions of photons that attenuated when passing through the glasses [27]. Consequently, it can assist in understanding the photon-attenuating trend for the oxyfluoride tellurite glasses. It has been proposed that the μ improves with increasing the density of the absorber [28]. The μ values for the oxyfluoride tellurite glasses are higher than that for the pure TeO_2 glass. For example, the μ values for the selected oxyfluoride tellurite glasses at 0.284 MeV are 1.211, 1.190, 1.177, 1.041, and 1.108 cm^{-1} for ZnFWTe1, ZnFWTe2, ZnFWTe3, ZnFWTe4, and ZnFWTe5 glasses, respectively. The μ for the pure TeO_2 glasses at this energy is 0.808 cm^{-1} .

For $E = 0.826$ MeV, the μ values are 0.406, 0.404, 0.406, 0.383, and 0.394 cm^{-1} , and 0.313 cm^{-1} for the pure TeO_2 sample. For all tested glasses (oxyfluoride tellurite glasses and pure TeO_2 glass), the maximum attenuation behavior is found at 0.284 MeV, due to the photoelectric effect. Correspondingly, due to this process, one can see that the μ reduces quickly between 0.284 MeV and 0.662 MeV. For instance, for ZnFWTe1 and ZnFWTe2 samples, the μ varied between 1.211–0.476 cm^{-1} and 1.190–0.473 cm^{-1} , respectively. Between 1.173–1.33 MeV, the Compton scattering becomes important, and, due to this process, the μ shows almost constant values with the increasing energy. For ZnFWTe1, the μ values are 0.324 cm^{-1} at 1.173 MeV, 0.309 cm^{-1} at 1.275 MeV, and 0.301 cm^{-1} at 1.33 MeV. From Figure 2, it could be observed that ZnFWTe1 has the highest μ at all considered energies. The glass ZnFWTe4 has the lowest μ among the oxyfluoride tellurite glasses. As expected, μ is a function of the density of the samples, whereby the μ shows a gradual increase

with increasing the density. This result is similar to the findings reported for different glasses [29,30].

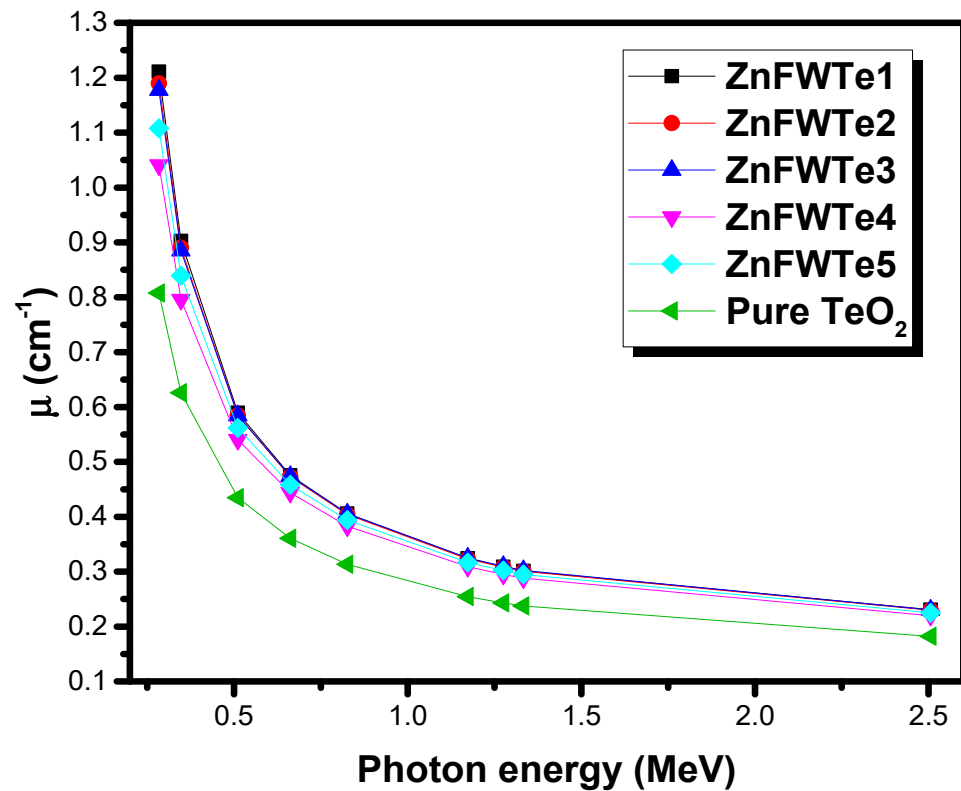


Figure 2. The linear attenuation coefficient for the selected oxyfluoride tellurite glasses.

Figure 3 shows the Z_{eff} for the oxyfluoride tellurite glasses between 0.284–2.506 MeV. Moreover, in this figure, the researcher included the Z_{eff} for the pure TeO_2 glass. As noted in the previous curves, the maximum Z_{eff} is found at 0.284 MeV and equals to 34.30, 33.42, 32.51, 30.94, 31.75, and 30.29 for ZnFWTe1, ZnFWTe2, ZnFWTe3, ZnFWTe4, ZnFWTe5, and pure TeO_2 glass, respectively. The high Z_{eff} at this energy is related to the photoelectric effect (PE), and the possibility of PE depends upon Z^{4-5} and has a considerable inverse relation with the energy. Largely, one can see that Z_{eff} decreases with energy except at 2.506 MeV. The Z_{eff} behavior with the energy can be divided as follows: (i) a quick decreasing in Z_{eff} between 0.284–0.662 MeV, (ii) a very slight decrease in Z_{eff} between 0.826–1.33 MeV and (iii) a slight increase in Z_{eff} , which occurs at the last energy only. For instance, for ZnFWTe1, the Z_{eff} in the previous three regions varied between 34.30–25.82, 25.32–23.57, and 23.57–24.47. Increasing the Z_{eff} in the last energy is related to pair production, as mentioned by Al-Hadeethi et al. [31].

Figure 4 presents the HVL for the chosen ZnFWTe1–ZnFWTe5 glasses and pure TeO_2 glass at the eight energies under study. The increase in the density of the sample modifies the radiation-shielding properties of the samples. As expected, from Figure 4, the HVL depends strongly on the density of the samples, where ZnFWTe1 with the highest density possesses the least HVL and vice versa. The HVL of the glasses shows a gradual decrease with increasing the density. Following these grounds, it was found that the pure TeO_2 has thicker HVL than the selected oxyfluoride tellurite glasses. At 0.284 MeV, the following values for the HVL were reported: 0.572, 0.583, 0.589, 0.666, and 0.626 cm for ZnFWTe1, ZnFWTe2, ZnFWTe3, ZnFWTe4, and ZnFWTe5. On the other hand, the HVL for pure TeO_2 at this energy was established to be 0.858 cm. Moreover, the HVL shows a gradual increase with increasing energy. For ZnFWTe2, the HVL changes from 0.583 to 3.018 cm between these energies. Meanwhile, for pure TeO_2 glass, the HVL changes from 0.858 to 3.808 cm. These results imply the weakening in the photons' attenuating ability of the samples along

with the increase in the energy of the photon. These results are consistent with those found earlier for different types of glasses [32,33].

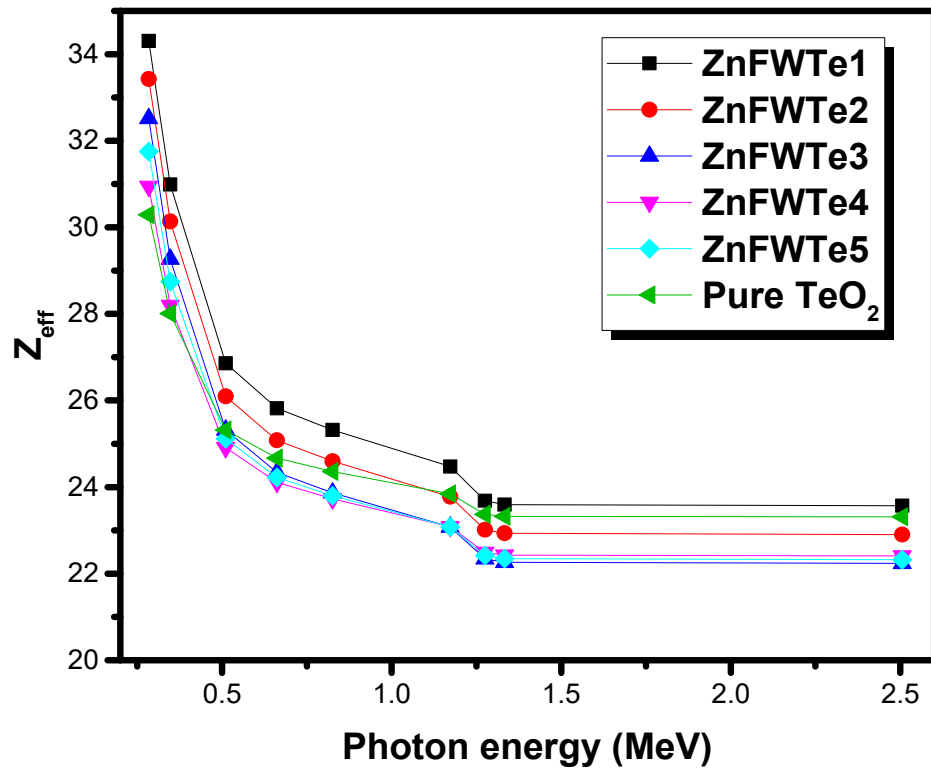


Figure 3. The effective atomic number for the selected oxyfluoride tellurite samples.

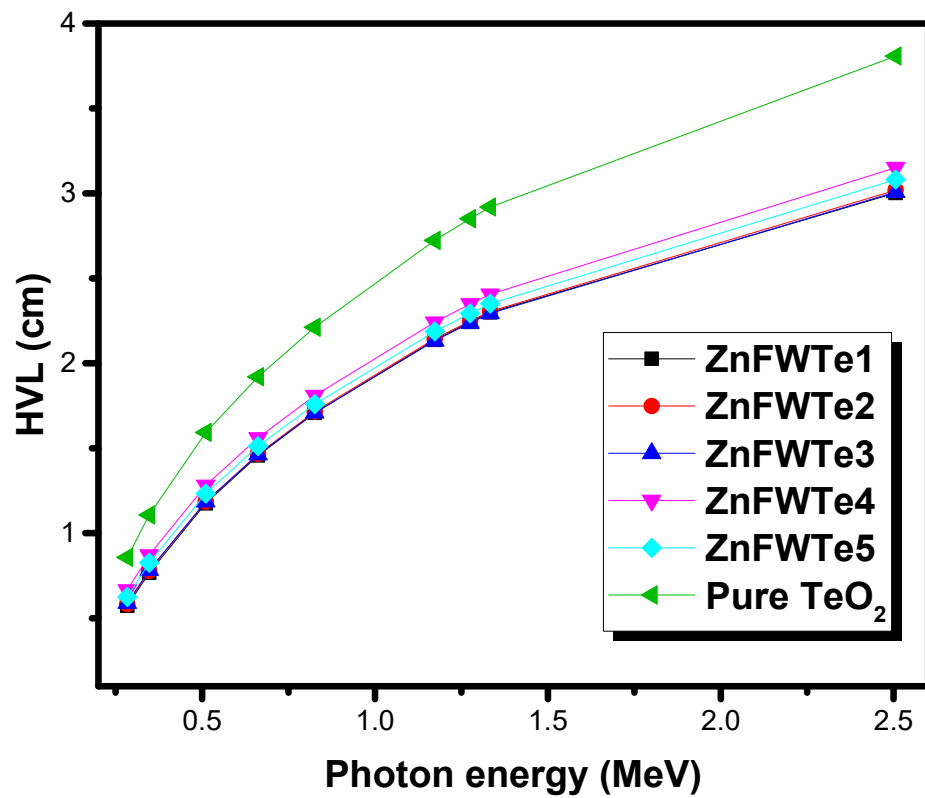


Figure 4. The half value layer for the selected oxyfluoride tellurite glasses.

Moreover, we evaluated the TVL for the oxyfluoride tellurite glasses. The researcher plotted the TVL results for ZnFWTe1-ZnFWTe5 glasses and pure TeO₂ glass at 0.284 and 0.347 MeV (as an example) in Figures 5 and 6, respectively. It can be noticed from both figures that as the density of the samples increased, the TVL reduced and thus the photons' shielding capability were enhanced. All the ZnFWTe1-ZnFWTe5 samples have a higher density than that of pure TeO₂. Consequently, they have lower TVL than pure TeO₂. This is correct at both energies, as represented in Figures 5 and 6 and also at the other energies (not shown in this work).

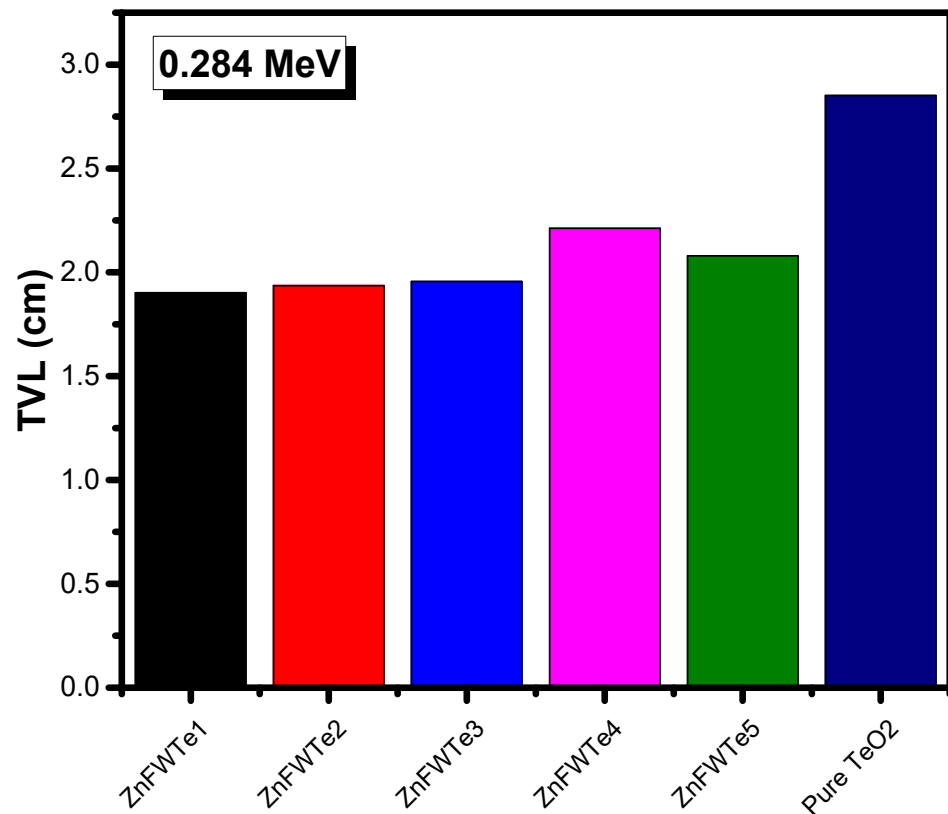


Figure 5. The tenth value layer for the selected oxyfluoride tellurite glasses at 0.284 MeV.

At 0.284 MeV, for instance, one requires a 1.901-cm thickness of the sample ZnFWTe1 to decrease its intensity to one-tenth of its original (i.e., TVL), whereas 1.936, 1.956, 2.212, and 2.079 cm are required for glasses ZnFWTe2, ZnFWTe3, ZnFWTe4, and ZnFWTe5, respectively. It will take about a 2.851-cm thickness of pure TeO₂ glass to achieve the same purpose. At 0.347 MeV, approximately a 2.550-cm thickness of ZnFWTe1 is required to reduce the incoming photons' level to one-tenth of the original level, while 2.587, 2.603, 2.894, and 2.744 cm are required for the samples ZnFWTe2, ZnFWTe3, ZnFWTe4, and ZnFWTe5, respectively. For the pure TeO₂ glass, a 3.678-cm thickness of this sample is required to achieve this aim. From these results, the researcher found that the TVL increases with the increasing energy.

Figure 7 illustrates the comparison between the MFP for the tested ZnFWTe1-ZnFWTe5 at 2.506 MeV with some common materials used for the radiation-shielding applications [34]. In general, it is expected that the MFP and μ should show an opposite trend to each other. This is true for the tested oxyfluoride tellurite glasses, as illustrated in Figure 7, whereby pure TeO₂ has a higher MFP than the present ZnFWTe1-ZnFWTe5 glasses. Moreover, the current glasses have lower MFP than ordinary concrete and the RS-360 and RS-253-G18 glasses.

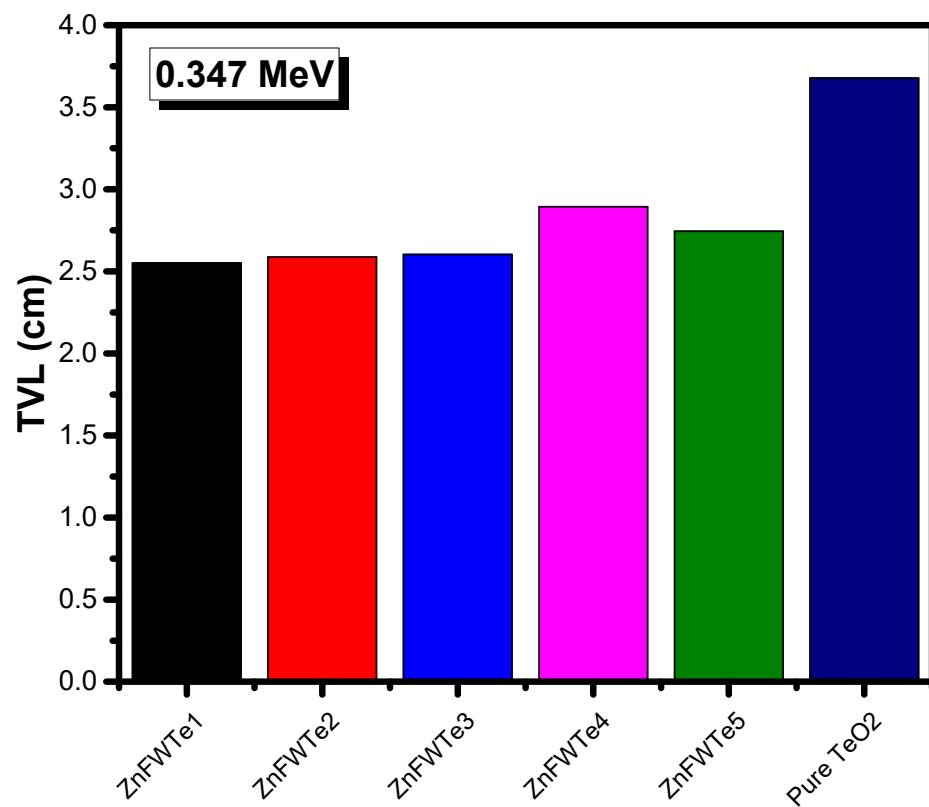


Figure 6. The tenth value layer for the selected oxyfluoride tellurite glasses at 0.347 MeV.

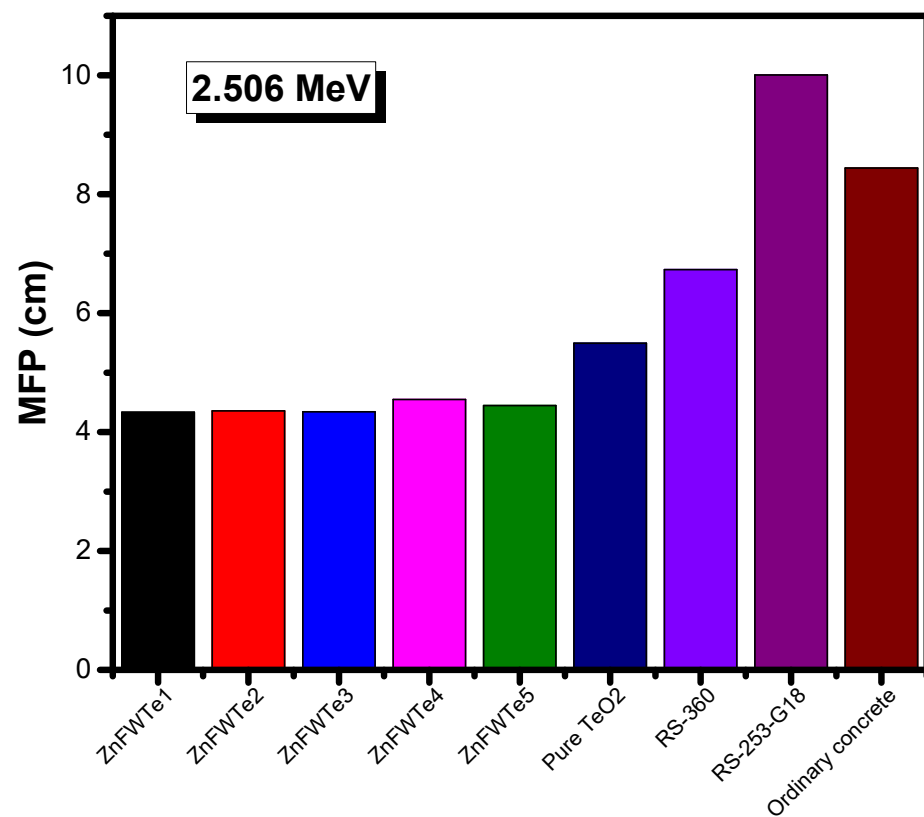


Figure 7. The mean free path for the selected oxyfluoride tellurite glasses at 2.506 MeV in comparison with other shielding materials.

The HVL for the selected TeO₂ glasses containing ZnF₂ and WO₃ at 0.347 MeV varied between 0.768 and 0.826 cm; this is lower than the HVL for 90.4 TeO₂–9.6 ZnO–4NiO glass, which is equal to 0.967 cm [35]. Moreover, the HVL for the present glasses are slightly lower than those of the ZnO–MoO₃–TeO₂ glasses [36]. Rammah et al. [37] found that the HVL TeO₂–Li₂O–ZnO glasses at 0.347 MeV varied between 1.039 and 1.12 cm and this is higher than the HVL for our present glasses. Ersundu et al. [38] studied the WO₃–MoO₃–TeO₂ glasses and for this glass system, the HVL is varied, at between 0.875 and 0.994 cm (at 0.347 MeV); thus, it shows a higher HVL than our present glasses. This confirms the possibility of developing the current glasses for radiation protection aims in the tested energy zone.

4. Conclusions

We reported the radiation shielding features of the ternary oxyfluoride tellurite glasses, WO₃–ZnF₂–TeO₂, using Phy-X/PSD software. A discussion and prediction were provided concerning the effect of the TeO₂, WO₃, and ZnF₂ on the attenuating performance of the tested glass system. The μ/ρ for the WO₃–ZnF₂–TeO₂ glasses highly depends on the concentration of WO₃, as well as on ZnF₂. All ZnFWTe1–ZnFWTe5 glasses have higher μ/ρ values than that of the pure TeO₂ glass at the selected energies. The replacement of TeO₂ by ZnF₂ in the samples with a fixed content of WO₃ increases the μ/ρ , as well as for the glasses with a fixed TeO₂ content. In contrast, the replacement of WO₃ by ZnF₂ led to a decline in the μ/ρ values. ZnFWTe4 has the lowest μ among the oxyfluoride tellurite glasses; however, it has a higher value of μ than pure TeO₂ glass. The maximum Z_{eff} is found at 0.284 MeV and varied between 31.75 and 34.30 for the tested glasses. The HVL of the current glasses shows a gradual decrease with the increasing density. The study found that the pure TeO₂ has a thicker HVL than the selected samples. We found that a 1.901-cm thickness of ZnFWTe1 is needed to reduce the intensity of the photons with the energy of 0.284 MeV to one-tenth of its original, whereas 1.936, 1.956, 2.212, and 2.079 cm are required for the glasses ZnFWTe2, ZnFWTe3, ZnFWTe4, and ZnFWTe5, respectively.

Author Contributions: Writing—original draft preparation: A.H.A. and M.I.S.; writing—review and editing; supervision; funding acquisition, A.H.A. and M.I.S.; Conceptualization; validation: A.H.A. and M.I.S.; methodology; investigation: A.H.A. and M.I.S.; project administration; A.H.A. All authors have read and agreed to the published version of the manuscript.

Funding: This work was funded by Princess Nourah bint Abdulrahman University.

Institutional Review Board Statement: Not applicable.

Informed Consent Statement: Not applicable.

Data Availability Statement: Not applicable.

Acknowledgments: The authors express their gratitude to Princess Nourah bint Abdulrahman University Researchers Supporting Project number (PNURSP2022R2), Princess Nourah bint Abdulrahman University, Riyadh, Saudi Arabia.

Conflicts of Interest: The authors declare no conflict of interest.

References

1. Dong, M.; Xue, X.; Yang, H.; Liu, D.; Wang, C.; Li, Z. A novel comprehensive utilization of vanadium slag: As gamma ray shielding material. *J. Hazard. Mater.* **2016**, *318*, 751–757. [[CrossRef](#)] [[PubMed](#)]
2. Dong, M.; Zhou, S.; Xue, X.; Feng, X.; Sayyed, M.I.; Khandaker, M.U.; Bradley, D.A. The potential use of boron containing resources for protection against nuclear radiation. *Radiat. Phys. Chem.* **2021**, *188*, 109601. [[CrossRef](#)]
3. Kavaz, E.; Ghanim, E.H.; Abouhaswa, A.S. Optical, structural and nuclear radiation security proper-ties of newly fabricated V2O5–SrO–PbO glass system. *J. Non-Cryst. Solids* **2020**, *538*, 120045. [[CrossRef](#)]
4. Araz, A.; Kavaz, E.; Durak, R. Neutron and photon shielding competences of aluminum open-cell foams filled with different epoxy mixtures: An experimental study. *Radiat. Phys. Chem.* **2021**, *182*, 109382. [[CrossRef](#)]
5. McCaffrey, J.P.; Shen, H.; Downton, B.; Mainegra-Hing, E. Radiation attenuation by lead and nonlead materials used in radiation shielding garments. *Med. Phys.* **2007**, *34*, 530–537. [[CrossRef](#)]

6. Mahmoud, K.; Sayyed, M.; Tashlykov, O. Gamma ray shielding characteristics and exposure buildup factor for some natural rocks using MCNP-5 code. *Nucl. Eng. Technol.* **2019**, *51*, 1835–1841. [[CrossRef](#)]
7. Khazaalah, T.H.; Mustafa, I.S.; Al-Ghamdi, H.; Rahman, A.A.; Sayyed, M.I.; Almuqrin, A.H.; Zaid, M.H.M.; Hisam, R.; Malik, M.F.I.A.; Ezra, N.S.; et al. The Effect of WO₃-Doped Soda Lime Silica SLS Waste Glass to Develop Lead-Free Glass as a Shielding Material against Radiation. *Sustainability* **2022**, *14*, 2413. [[CrossRef](#)]
8. Abouhaswa, A.S.; Kavaz, E. A novel B₂O₃-Na₂O-BaO-HgO glass system: Synthesis, physical, optical and nuclear shielding features. *Ceram. Int.* **2020**, *46*, 16166–16177. [[CrossRef](#)]
9. Abouhaswa, A.S.; Kavaz, E. Bi₂O₃ effect on physical, optical, structural and radiation safety characteristics of B₂O₃-Na₂O-ZnO-CaO glass system. *J. Non-Cryst. Solids* **2020**, *535*, 119993. [[CrossRef](#)]
10. Akyildirim, H.; Kavaz, E.; El-Agawany, F.; Yousef, E.S.S.; Rammah, Y. Radiation shielding features of zirconolite silicate glasses using XCOM and FLUKA simulation code. *J. Non-Cryst. Solids* **2020**, *545*, 120245. [[CrossRef](#)]
11. Kavaz, E.; Ekinci, N.; Tekin, H.O.; Sayyed, M.I.; Aygün, B.; Perişanoğlu, U. Estimation of gamma radiation shielding qualification of newly developed glasses by using WinXCOM and MCNPX code. *Prog. Nucl. Energy* **2019**, *115*, 12–20. [[CrossRef](#)]
12. Singh, V.P.; Badiger, N.M. Shielding efficiency of lead borate and nickel borate glasses for gamma rays and neutrons. *Glas. Phys. Chem.* **2015**, *41*, 276–283. [[CrossRef](#)]
13. Chanthima, N.; Kaewkhao, J.; Limkitjaroenporn, P.; Tuscharoen, S.; Kothan, S.; Tungjai, M.; Kaewjaeng, S.; Sarachai, S.; Limsuwan, P. Development of BaO–ZnO–B₂O₃ glasses as a radiation shielding material. *Radiat. Phys. Chem.* **2017**, *137*, 72–77. [[CrossRef](#)]
14. Kaewjaeng, S.; Kothan, S.; Chaiphaksa, W.; Chanthima, N.; Rajaramkrishna, R.; Kim, H.J.; Kaewkhao, J. High transparency La₂O₃-CaO-B₂O₃-SiO₂ glass for diagnosis x-rays shielding material application. *Radiat. Phys. Chem.* **2019**, *160*, 41–47. [[CrossRef](#)]
15. Kurudirek, M. Radiation shielding and effective atomic number studies in different types of shielding concretes, lead base and non-lead base glass systems for total electron interaction: A comparative study. *Nucl. Eng. Des.* **2014**, *280*, 440–448. [[CrossRef](#)]
16. Cheewasukhanont, W.; Limkitjaroenporn, P.; Sayyed, M.; Kothan, S.; Kim, H.; Kaewkhao, J. High density of tungsten gadolinium borate glasses for radiation shielding material: Effect of WO₃ concentration. *Radiat. Phys. Chem.* **2021**, *192*, 109926. [[CrossRef](#)]
17. Kirdsiri, K.; Kaewkhao, J.; Chanthima, N.; Limsuwan, P. Comparative study of silicate glasses containing Bi₂O₃, PbO and BaO: Radiation shielding and optical properties. *Ann. Nucl. Energy* **2011**, *38*, 1438–1441. [[CrossRef](#)]
18. Kaur, P.; Singh, K.; Thakur, S.; Kurudirek, M.; Rafiei, M.M. Structural investigations and nuclear radiation shielding ability of bismuth lithium antimony borate glasses. *J. Phys. Chem. Solids* **2021**, *150*, 109812. [[CrossRef](#)]
19. El-Moneim, A.A. Effect of ZnF₂ and WO₃ on elastic properties of oxyfluoride tellurite ZnF₂-WO₃-TeO₂ glasses: Theoretical analysis. *Chin. J. Phys.* **2020**, *65*, 412–423. [[CrossRef](#)]
20. Bagheri, R.; Moghaddam, A.K.; Shirmardi, S.P.; Azadbakht, B.; Salehi, M. Determination of gamma-ray shielding properties for silicate glasses containing Bi₂O₃, PbO, and BaO. *J. Non-Cryst. Solids* **2018**, *479*, 62–71. [[CrossRef](#)]
21. Chanthima, N.; Kaewkhao, J. Investigation on radiation shielding parameters of bismuth borosilicate glass from 1 keV to 100 GeV. *Ann. Nucl. Energy* **2013**, *55*, 23–28. [[CrossRef](#)]
22. El-Khayatt, A.; Ali, A.; Singh, V.P. Photon attenuation coefficients of Heavy-Metal Oxide glasses by MCNP code, XCOM program and experimental data: A comparison study. *Nucl. Instruments Methods Phys. Res. Sect. A Accel. Spectrom. Detect. Assoc. Equip.* **2014**, *735*, 207–212. [[CrossRef](#)]
23. Al-Buriah, M.S.; Rammah, Y.S. Electronic polarizability, dielectric, and gamma-ray shielding properties of some tellurite-based glasses. *Appl. Phys. A* **2019**, *125*, 678. [[CrossRef](#)]
24. Sayyed, M.I.; Laariedh, F.; Kumr, A.; Al Buriah, M.S. Experimental studies on the gamma photons shielding competence of TeO₂-PbO-BaO-Na₂O-B₂O₃ glasses. *Appl. Phys. A* **2020**, *126*, 4. [[CrossRef](#)]
25. Şakar, E.; Özpölat, Ö.F.; Alım, B.; Sayyed, M.; Kurudirek, M. Phy-X / PSD: Development of a user friendly online software for calculation of parameters relevant to radiation shielding and dosimetry. *Radiat. Phys. Chem.* **2020**, *166*, 108496. [[CrossRef](#)]
26. Yousef, E.S.S. Characterization of oxyfluoride tellurite glasses through thermal, optical and ultrasonic measurements. *J. Phys. D Appl. Phys.* **2005**, *38*, 3970–3975. [[CrossRef](#)]
27. Sayyed, M.I.; Elmahroug, Y.; Elbashir, B.O.; Issa, S. Gamma-ray shielding properties of zinc oxide soda lime silica glasses. *J. Mater. Sci. Mater. Electron.* **2017**, *28*, 4064–4074. [[CrossRef](#)]
28. Al-Hadeethi, Y.; Sayyed, M.I. Radiation attenuation properties of Bi₂O₃-Na₂O-V₂O₅-TiO₂-TeO₂ glass system using Phy-X/ PSD software. *Ceram. Int.* **2020**, *46*, 4795–4800. [[CrossRef](#)]
29. Cheewasukhanont, W.; Limkitjaroenporn, P.; Kothan, S.; Kedkaew, C.; Kaewkhao, J. The effect of particle size on radiation shielding properties for bismuth borosilicate glass. *Radiat. Phys. Chem.* **2020**, *172*, 108791. [[CrossRef](#)]
30. Issa, S.A.; Saddeek, Y.; Sayyed, M.; Tekin, H.O.; Kilicoglu, O. Radiation shielding features using MCNPX code and mechanical properties of the PbO Na₂O B₂O₃CaO Al₂O₃SiO₂ glass systems. *Compos. Part B Eng.* **2019**, *167*, 231–240. [[CrossRef](#)]
31. Al Hadeethi, Y.; Sayyed, M.I.; Kaewkhao, J.; Askin, A.; Rafah, B.M.; Mkawi, E.M.; Rajaramkrishna, R. Physical, structural, optical, and radiation shielding properties of B₂O₃-Gd₂O₃-Y₂O₃ glass system. *Appl. Phys. A* **2019**, *125*, 852. [[CrossRef](#)]
32. Kamislioglu, M. An investigation into gamma radiation shielding parameters of the (Al:Si) and (Al+Na):Si-doped international simple glasses (ISG) used in nuclear waste management, deploying Phy-X/PSD and SRIM software. *J. Mater. Sci. Mater. Electron.* **2021**, *32*, 12690–12704. [[CrossRef](#)]

33. Rajesh, M.; Kavaz, E.; Deva Prasad Raju, B. Photoluminescence, radiative shielding properties of Sm^{3+} ions doped fluoroborosilicate glasses for visible (reddish-orange) display and radiation shielding applications. *Mater. Res. Bull.* **2021**, *142*, 111383. [[CrossRef](#)]
34. Kaur, P.; Singh, K.J.; Thakur, S.; Singh, P.; Bajwa, B.S. Investigation of bismuth borate glass system modified with barium for structural and gamma-ray shielding properties. *Spectrochim. Acta Part A Mol. Biomol. Spectrosc.* **2019**, *206*, 367–377. [[CrossRef](#)]
35. Al-Buriahi, M.S.; Bakhsh, E.M.; Tonguc, B.; Bahadar Khan, S. Mechanical and radiation shielding properties of tellurite glasses doped with ZnO and NiO. *Ceram. Inter-Natl.* **2020**, *46*, 19078–19083. [[CrossRef](#)]
36. Ersundu, M.C.; Ersundu, A.E.; Gedikoğlu, N.; Şakar, E.; Büyükyıldız, M.; Kurudirek, M. Physical, mechanical and gamma-ray shielding properties of highly transparent ZnO-MoO₃-TeO₂ glasses. *J. Non-Cryst. Solids* **2019**, *524*, 119648. [[CrossRef](#)]
37. Rammah, Y.; El-Agwany, F.; Mahmoud, K.; Novatski, A.; El-Mallawany, R. Role of ZnO on TeO₂-Li₂O-ZnO glasses for optical and nuclear radiation shielding applications utilizing MCNP5 simulations and WINXCOM program. *J. Non-Cryst. Solids* **2020**, *544*, 120162. [[CrossRef](#)]
38. Ersundu, A.E.; Büyükyıldız, M.; Ersundu, M.C.; Şakar, E.; Kurudirek, M. The heavy metal oxide glasses within the WO₃-MoO₃-TeO₂ system to investigate the shielding properties of radiation applications. *Prog. Nucl. Energy* **2018**, *104*, 280–287. [[CrossRef](#)]